

Scale-dependent covariance of soil physical properties above and below a soil horizon interface: Pedogenic versus anthropogenic influences on total porosity

M. F. Dyck¹ and R. G. Kachanoski²

¹*Department of Renewable Resources, University of Alberta, Edmonton, Alberta, Canada T6G 2E3 (e-mail: miles.dyck@ualberta.ca); and* ²*Memorial University of Newfoundland, St. John's, Newfoundland, Canada A1C 5S7. Received 30 June 2010, accepted 19 January 2011.*

Dyck, M. F. and Kachanoski, R. G. 2011. **Scale-dependent covariance of soil physical properties above and below a soil horizon interface: Pedogenic versus anthropogenic influences on total porosity.** *Can. J. Soil Sci.* **91**: 149–159. The basic unit of soil – the pedon – is described as the minimum, three-dimensional unit of soil representative of the variability of soil horizon dimensions and morphology. Pedogenic processes responsible for soil horizon and soil profile formation are primarily hydrologic in nature. The spatially variable distribution of soil horizons (i.e., the variation among pedons within catenae or landscapes) is likely a reflection of the inherent variability of the soil parent material and the spatial variability of hydrological/pedogenic processes. This paper explores the spatial variability and spatially scale-dependent covariance between a basic soil property (porosity) above and below an A/B horizon interface under adjacent disturbed (cultivated) and undisturbed (forested) conditions. A combination of scale-dependent variance and Fourier-domain spectral analysis shows that the scale-dependent covariance of A and B horizon porosity varies significantly between the cultivated and forested sampling transects. The majority of these observed differences between the scale-dependent covariance of A and B horizon porosity under contrasting land uses is attributed to tillage. These results suggest that anthropogenic activities such as tillage may not only alter the surface horizons, but the nature of the spatial covariance between surface and underlying horizons which likely influences current soil hydrological processes.

Key words: Porosity, tillage, pedon, spectral analysis

Dyck, M. F. et Kachanoski, R. G. 2011. **La covariance influencée par l'échelle des propriétés physiques du sol au-dessus et en-dessous de l'interface des horizons: incidences pédogénétiques et anthropiques sur la porosité globale.** *Can. J. Soil Sci.* **91**: 149–159. L'unité de base du sol – le pédon – correspond à la plus petite unité tridimensionnelle du sol représentative de la variabilité de l'horizon sur les plans dimensionnel et morphologique (Agriculture et Agroalimentaire Canada, 1998). Les phénomènes pédogénétiques qui expliquent la formation de l'horizon et du profil du sol sont essentiellement de nature hydrologique. Le fait que la distribution des horizons varie dans l'espace (à savoir, répartition des pédons dans la caténa ou le relief) reflète sans doute la variabilité inhérente des matériaux d'origine et la variabilité spatiale des processus hydrologiques/pédogénétiques. Cet article explore la variabilité spatiale et la covariance spatiale influencée par l'échelle d'une propriété fondamentale du sol (porosité) au-dessus et en-dessous de l'interface des horizons A/B, dans un sol adjacent intact (boisé) ou perturbé (cultivé). L'analyse de la variance influencée par l'échelle (van Weesenbeeck et Kachanoski, 1991) et l'analyse spectrale du domaine de Fourier révèlent que la covariance influencée par l'échelle de la porosité des horizons A et B varie sensiblement le long des transects d'échantillonnage pour les sols cultivé et boisé. L'écart entre la covariance influencée par l'échelle de la porosité des horizons A et B dans les sols à vocation contrastante dérive en grande partie du travail du sol. Ces résultats laissent croire que les activités anthropiques comme les labours peuvent non seulement altérer les horizons de surface, mais la nature même de la covariance spatiale entre les horizons de surface et ceux qu'ils surmontent, ce qui exerce sans doute une influence sur l'hydrologie du sol.

Mots clés: Porosité, travail du sol, pédon, analyse spectrale

The nature and structure of soil pore networks (i.e., total pore volume, pore size distribution, tortuosity and connectivity) have been influenced by complex sedimentary processes during parent material deposition, subsequent pedogenesis and anthropogenic and biological activities. Depositional processes establish a soil's texture and mineralogy. Pedogenic processes subsequently alter the parent material. Soil structure and soil horizons are the most obvious expressions of these pedogenic alterations. Anthropogenic and biological activities, such as tillage and bioturbation, further alter soil properties and pore geometry.

The basic unit of soil, the pedon, is described as the minimum, three-dimensional unit of soil representative of the variability of soil horizon dimensions and morphology (Agriculture and Agri-Food Canada 1998). Pedogenic processes responsible for soil horizon formation, such as translocation of solutes and colloids, are hydrological in nature, which may also alter the pore geometry, and, therefore, hydraulic properties of the soil. Therefore, the pedon and the distribution of pedons over catenae and landscapes is the result of complex interactions and feedbacks between hydrological, pedogenic, anthropogenic and biological processes (Lin et al. 2008).

In hydrology, the representative elementary volume is the macroscopic scale at which pore-scale variations are consistently captured to yield consistent average hydraulic properties (e.g., porosity, hydraulic conductivity). It is unclear whether the scale of the representative elementary volume is related to the scale of the pedon, but Dyck and Kachanoski (2010) showed that the pedon scale is hydrologically significant. Most soils have at least two horizons separated by a horizon interface. Because soil horizons (e.g., A and B horizons) have different average hydraulic properties and their boundaries are visually distinct, it is often assumed that soil horizons are independent layers and that the interface between soil horizons has no influence on the hydraulic behavior of the entire soil profile. But, as indicated above, interactions between hydrological, pedogenic, anthropogenic and biological processes have: (1) created spatially variable soil horizons and soil horizon interfaces; (2) modified the pore structure within soil horizons such that average hydraulic properties of individual horizons are different (but may be only modestly so); and (3) as a result of (1) and (2), likely created a scale-dependent (quite possibly temporally dependent), spatial covariance between the hydraulic properties of individual, overlying horizons.

Major contributions to flow and transport theory in spatially variable, vertically heterogeneous soils are presented in stochastic stream tube (i.e., Jury and Utterman 1992) or stochastic continuum frameworks (i.e., Yeh et al. 1985a, b, c) or via numerical simulations models on generated random fields of hydraulic properties (e.g., Roth, 1995; Ursino et al. 2000). Recent, comprehensive reviews of stream tube and stochastic continuum frameworks are available (Vanderborght et al. 2006; Vereecken et al. 2007). An important result of stochastic continuum investigations is that the horizontal and vertical covariance structure of soil pore geometry at the micro-scale influences hydraulic properties at small scales (i.e., representative elementary volume scale; Ursino et al. 2000), which, in turn, significantly influence large scale flow and transport behavior (i.e., pedon or field scale; Yeh et al. 1985a, b, c). Therefore, quantifying the complex spatial covariance between soil physical and hydraulic properties in overlying horizons is desirable because: (1) Spatial patterns of soil physical and hydraulic properties are the result of the complex interactions of sedimentary, hydrological, pedogenic, anthropogenic, and biological processes up to the time of observation. Characterization of the horizontal and vertical covariance structure of soil physical and hydraulic properties may illuminate the nature and mechanisms of the interactions between the various processes responsible for the spatial variability. (2) Quantification and mitigation of the environmental risks associated with the aqueous transport of contaminants introduced into the soil requires characterization of the horizontal and vertical covariance structure of soil physical and hydraulic properties.

Studies of the spatial variability of soil porosity and bulk density have largely concentrated on surface soil properties under various tillage regimes (Carter 1995; Alletto and Coquette 2009). The objective of this paper is to quantify and interpret the scale-dependent spatial variance and covariance of soil porosity (a primary soil physical property) above and below a soil horizon interface for adjacent natural (forested) and cultivated soils developed on the same parent material.

MATERIALS AND METHODS

Soil Sampling and Site Description

The site is located on the Delhi Agricultural Research Station in Southern Ontario, Canada, and was selected for its general uniformity in topography over the study area (<1% slope). The soil at the site is a Fox series (Brunisolic Grey Brown Luvisol) with a loamy sand texture. The dataset analyzed in this paper is part of a larger dataset summarized by Protz et al. (1987). The spatial variability and autocorrelation structure of the soil horizon dimensions at this site has been previously described by Kachanoski (1988). Soil samples were collected above and below the A/B1 horizon interface from sampling transects under virgin forest (undisturbed) and cultivated fields. Each transect was 100-m long and was sampled every meter. Within each 100-m transect, a 10-m transect was sampled every 0.1-m. Soil samples were extracted with a core that was pushed into the face of a trench excavated with a backhoe. Each sample was oven-dried and bulk density was calculated based on the oven-dry weight and the calculated volume of the sample. Porosity was then calculated using the estimated bulk density and an assumed particle density of 2.65 g cm^{-3} .

Spectral Analysis

Any series of discrete measurements of a variable, X that varies in time or space may be described as a stochastic process (Gelhar 1993), where each observation in time or space, X_t ($t = 1 \dots N$) is considered a realization of the joint probability distribution of the process. The spectral, Fourier domain representation of a discrete, equally-spaced, zero mean, second order stationary, stochastic process, X_t is expressed by the spectral representation theorem for a stationary process (Percival and Walden 1993):

$$X_t = \int_{-1/2}^{1/2} e^{i2\pi ft} dZ(f) \quad (1)$$

where X_t is t th observation of the process, f is the Fourier frequency ($|f| \leq 1/2$), $i = \sqrt{-1}$, and $dZ(f)$ are random amplitudes and phases. Recalling Euler's formula that $e^{i2\pi ft}$ can be expressed as a sum of sine and cosine functions, $dZ(f)$ are the amplitudes of the sine (out of phase, imaginary) and cosine (in phase, real)

components of the signal. The variance of the process, X_t , at each frequency, f , is quantified with the power spectrum, defined as (Percival and Walden 1993):

$$S_{XX}(f) = \frac{d}{df} S_{XX}^{(l)}(f) \quad (2)$$

where $S_{XX}^{(l)}(f) = E\{|dZ(f)|^2\}$, which is called the integrated spectrum. The operator, $|\cdot|^2$ represents the squared modulus of a complex number (i.e., $|a|^2 = a^*a$ where the asterisk represents the complex conjugate). Power spectra partition the total variance of a process into $N/2$ independent estimates of variance at each spatial frequency, f ($f = K/N$; $K = 1, 2 \dots N/2$; for a real valued series the variance at positive and negative frequencies are equal so only the positive frequencies are considered). The shape of the power spectrum of a spatial series is an indicator of the spatial autocovariance structure (Duffy and Gelhar 1985). For example, a purely random spatial pattern will have a constant power spectrum value at each spatial frequency, whereas nonrandom spatial patterns will have significantly different power spectrum values at individual frequencies or bands of frequencies.

Spectral coherency analysis is used to quantify the scale-dependent linear relationship between two series, X_t and Y_t (Kachanoski and de Jong 1988). Covariance between two spatial series as a function of spatial scale is quantified with the cross spectrum:

$$S_{XY}(f) = S_{XX}(f)S_{YY}^*(f) \quad (3)$$

The cross spectrum consists of in-phase and out-of-phase covariance components:

$$S_{XY}(f) = C_{XY}(f) - iQ_{XY}(f) \quad (4)$$

where $C_{XY}(f)$ is the cospectrum (in-phase covariance) and $Q_{XY}(f)$ is the quadrature spectrum (out-of-phase covariance). The linear coefficient of determination describing the proportion of variance of series X_t explained by series Y_t as a function of spatial scale is then quantified with the squared coherency spectrum, $R_{XY}(f)$:

$$R_{XY}(f) = \frac{|S_{XY}(f)|^2}{S_{XX}(f)S_{YY}(f)} \quad (5)$$

Conventional estimates of variance and covariance of spatial series yield only the integrated power spectrum and in-phase cospectrum. Spectral analysis partitions the variance and covariance into orthogonal (statistically independent) Fourier frequencies (or period/scale, being the inverse of frequency). Thus, spectral analysis is an appropriate tool for quantifying spatially scale-dependent features of soil physical and hydraulic properties.

The resulting data set for this paper consisted of eight spatial series: porosity estimates for two horizons (A and B) taken from two transects (10- and 100-m) at two

different sites (forested and cultivated). Power spectra for each spatial series/signal, X , were estimated with the discrete Fourier transform by:

$$\begin{aligned} \hat{S}_{XX}(f_K) &= \langle \hat{S}_{XX}^{(p)}(f_K) \rangle \\ &= \frac{1}{2m+1} \sum_{j=-m}^m \left[\frac{1}{N} \left| \sum_{t=1}^N X_n e^{-2\pi i f_K t} \right|^2 \right] \end{aligned} \quad (6)$$

where $f_K = K/N$ ($K = 1, 2 \dots N/2$), $\hat{S}_{XX}(f_K)$ is the estimated power spectrum of series X , $\hat{S}_{XX}^{(p)}(f_K)$ is the periodogram, and $\langle \cdot \rangle$ denotes the expectation operator. The periodogram, $\hat{S}_{XX}^{(p)}(f_K)$, is a naïve estimator (i.e., only 2 degrees of freedom per estimated value) of the power spectrum, and therefore must be averaged (m-point moving average for this example). Spatial frequencies range between $1/N\Delta x$ to $1/2\Delta x$ corresponding to maximum spatial periods/scales of $N\Delta x$ (the transect length) to a minimum spatial period/scale of $2\Delta x$ (twice the sampling interval).

Cross spectra, $\hat{S}_{XY}(f_K)$, were estimated by:

$$\begin{aligned} \hat{S}_{XY}(f_K) &= \langle \hat{S}_{XX}^{(p)}(f_K) \hat{S}_{YY}^{(p)*}(f_K) \rangle \\ &= \frac{1}{2m+1} \sum_{j=-m}^m [\hat{S}_{XX}^{(p)}(f_{K+j}) \hat{S}_{YY}^{(p)*}(f_{K+j})] \end{aligned} \quad (7)$$

Where $\hat{S}_{XX}^{(p)}(f_K)$ and $\hat{S}_{YY}^{(p)}(f_K)$ are the periodograms of the X and Y spatial series (i.e., A and B horizon porosities), respectively (calculated with Eq. 6), * denotes the complex conjugate and m is the moving average index. As indicated in Eq. 4, the estimated cross spectrum real and imaginary components correspond to in phase $[C_{XY}(f_K)]$ and out of phase $[Q_{XY}(f_K)]$ covariance between series X and Y as a function of spatial frequency, respectively. Estimates of the coherency spectra are calculated by substitution of $\hat{S}_{XY}(f_K)$, $\hat{S}_{XX}(f_K)$ and $\hat{S}_{YY}(f_K)$ into Eq. 5.

As in Shumway (1988), for example, the $1-\alpha/2$ confidence interval for the power spectrum estimate at each frequency may be calculated with the chi-squared distribution:

$$\begin{aligned} \log[\hat{S}_{XX}(f)] - \log \left[\frac{\chi_{v,\alpha/2}^2}{v} \right] &\leq \log[\hat{S}_{XX}(f)] \\ &\leq \log[\hat{S}_{XX}(f)] - \log \left[\frac{\chi_{v,1-\alpha/2}^2}{v} \right] \end{aligned} \quad (8)$$

where $\chi_{v,\alpha/2}^2$ and $\chi_{v,1-\alpha/2}^2$ are the values of the chi-squared distribution with v degrees of freedom at $\alpha/2$ and $1-\alpha/2$ probabilities. In accordance with Brillinger (1981), Kachanoski et al. (1985), and Si (2008), the critical value for $\hat{R}_{XY}(f)$ is:

$$\rho_{XY} = 1 - (1 - \alpha)^{2/(v-2)} \quad (9)$$

For the moving average smoothing shown above, spectral estimates at each frequency have $2 \cdot (2m+1)$ degrees of freedom. For this dataset, $m=2$, giving 10 degrees of freedom.

Analysis of Stationarity and Scale Dependent Variance

The spectral representation theorem stated in Eq. 1 requires that the spatial series be second order stationary. A practical definition of second order stationarity is that the mean and variance of n ($n > 1$) equal length, equally spaced subsets of a spatial process are finite and equal (Percival and Walden 1993). Stationarity for autocorrelated spatial processes is a function of scale. For example, the variance of an autocorrelated process increases with increasing scale until a sill (autocorrelation length scale) is reached. The stationary variance of a spatial process or spatial series, then, cannot be estimated unless it is sampled at a scale greater than its autocorrelation length.

van Wesenbeeck and Kachanoski (1991) outline a method to estimate the scale at which the variance of a process does not change appreciably. Again, given a spatial series, X , of length, N sampled at equal intervals, the average variance of L subsets of X , comprised of observations that are within L sampling intervals of each other is:

$$Var_L(X) = E(V_L) \quad L = 1 \dots N - 1 \quad (10)$$

where $Var_L(X)$ is the variance of series, X at spatial scale $L \cdot \Delta x$, $E(\cdot)$ is the expectation operator, N is the number of observations in the series, and V_L is:

$$V_L = E((X_j - \bar{X}_L)^2) \quad j = \ell \dots \ell + L \quad (11)$$

$$\ell = 1 \dots N - L$$

and

$$\bar{X}_L = E(X_j) \quad (12)$$

Plots of $Var_L(X)$ versus $L \cdot \Delta x$ have shapes similar to variograms, although this calculation is not a variogram. Further, if a plots of $Var_L(X)$ versus $L \cdot \Delta x$ reach a sill (i.e., the variance does not change over many scales), it may be concluded that the transect length was adequate to estimate the stationary variance of the process.

RESULTS

Spatial series of the forested and cultivated 10- and 100-m sampling transects are presented in Figs. 1 and 2, respectively. Descriptive statistics for A and B horizon porosity for the 10- and 100-m transects in forested and cultivated sites are presented in Table 1. For all transects, the arithmetic mean, median and mode of the spatial series of porosity are almost equal indicating normally distributed, non-skewed probability distributions. For all series, estimated variance of the 100-m transects are on the order of two times larger than that of the 10-m transects, except for the cultivated A horizon. Variance estimates for 10- and 100-m sampling transects of the cultivated A horizon are almost equal.

Scale-dependent variance estimated with Eqs. 10 through 12 is presented in Fig. 3 for the 10- and 100-m forested transects and Fig. 4 for the 10- and 100-m cultivated transects. The shape of the scale-dependent variance graphs are similar for the forested A and B horizons and cultivated B horizon (Fig. 3A, 3B and 4B). For these examples (Fig. 3A, 3B, and 4B), the scale-dependent variance of the 100-m transects appears to continue increasing after the variance of the 10-m transects starts to decrease. Although the variance of the 10-m transects (Fig. 3A, 3B, and 4B) appears to reach a sill between the 5- and 7-m scales, the variance at these scales calculated with data from the 100-m transect is

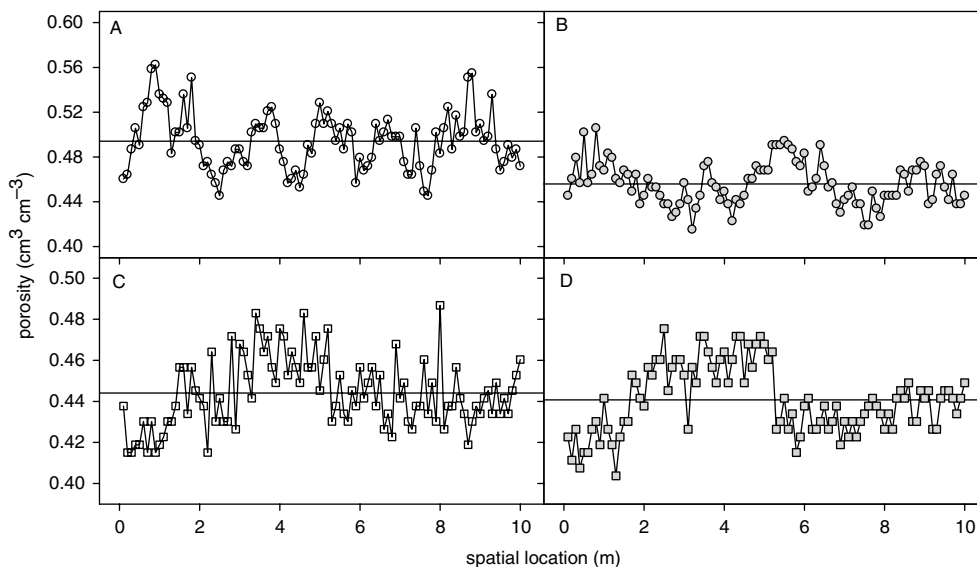


Fig. 1. Spatial series of porosity estimates for the 10-m nested transects: (A) forest A horizon; (B) forest B horizon; (C) cultivated A horizon; and (D) cultivated B horizon.

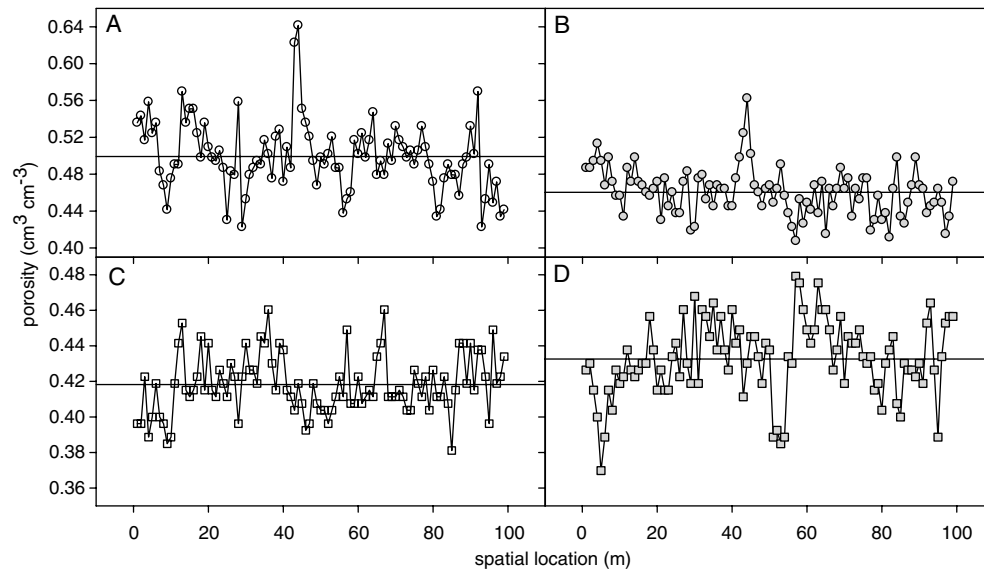


Fig. 2. Spatial series of porosity estimates for the 100-m transects: (A) forest A horizon; (B) forest B horizon; (C) cultivated A horizon; and (D) cultivated B horizon.

much greater. Therefore, it would appear that the 10-m nested transects are not representative of the larger 100-m transects. For example, a variance estimate at the 8-m scale calculated with data from a 10-m transect is the average of 20 variance estimates from 20 subsets of 81 data points within 8 m of each other over a total length of 10 m. A variance estimate at the 8-m scale calculated with data from a 100-m transect, however, is the average of 92 variance estimates from 92 subsets of 9 data points within 8 m of each other over a total length of 100 m. Because of the smaller sampling interval, more data points are in each 8-m subset of the 10-m transect, but the total number of 8-m subsets is smaller and taken over a smaller total distance than the 100-m transect. Subsequently, for these examples, the spatial structure of the 10-m nested transect may be representative of the process at small scales <5-m, but diverge from the 100-m transects at scales >5 m because the range in porosity at scales >5 m of the 100-m transects are not represented at these scales in the 10-m transects.

For the cultivated A horizon (Fig. 4A), the shapes of the scale-dependent variance of the 10- and 100-m transects are completely distinct. In this case, the total variance of the 10-m cultivated A horizon transect was slightly larger than the 100-m transect, but as Fig. 4A shows, this 10-m transect is not representative of the small scale variance structure as calculated with the porosity values from the 100-m transect and does not reach a sill. It would appear, therefore, that this 10-m transect was located on a portion of the 100-m transect with large local variability, whereas other sections of the 100-m transect must have much smaller local variability. Furthermore, the structure of the scale-dependent variance of the 100-m cultivated A horizon transect (Fig. 4A) is also slightly different from the structure of the rest of the 100-m transects (Figs. 3A, 3B and 4B). Specifically, the variance of the cultivated A horizon transect (Fig. 4A) does not reach a sill until the 70-m spatial scale, whereas other transects reach a sill at 40 m. This suggests that the 100-m cultivated A horizon has a

Table 1. Descriptive statistics of A and B horizon porosity estimates in forested and cultivated landscapes

Statistic ^z	Forest				Cultivated			
	A 100-m	B 100-m	A 10-m	B 10-m	A 100-m	B 100-m	A 10-m	B 10-m
Mean ^z	0.50	0.46	0.49	0.46	0.42	0.43	0.44	0.44
Variance ($\times 10^{-3}$) ^y	1.46	0.68	0.68	0.37	0.28	0.46	0.29	0.28
Minimum ^z	0.42	0.41	0.45	0.42	0.38	0.37	0.42	0.40
Maximum ^z	0.64	0.56	0.56	0.51	0.46	0.48	0.49	0.48
Median ^z	0.50	0.46	0.49	0.45	0.42	0.43	0.44	0.44
Mode ^z	0.49	0.46	0.49	0.44	0.41	0.43	0.43	0.43

^zUnits: $\text{cm}^3 \text{cm}^{-3}$.
^yUnits: $\text{cm}^6 \text{cm}^{-6}$.

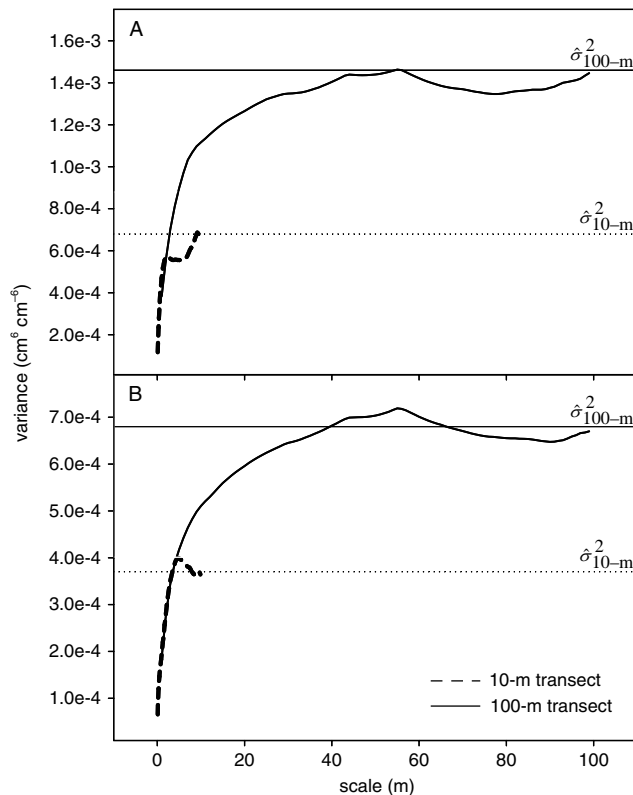


Fig. 3. Scale-dependent porosity variance of forested 10- and 100-m transects.

larger auto-correlation length scale than the other transects.

Based on the comparison of the scale-dependent variance of the 10-m and 100-m transects, it would appear that the 10-m nested transects do not capture the spatial variance structure of the porosity estimates that the 100-m transects do. The forested transects and the cultivated B horizon variance structures (Figs. 3A, 3B and 4B) show examples where the 10-m transects are representative of the local, small scale variance. The 10-m transects from these examples may be deemed non-stationary because they represent scales less than the autocorrelation length scale. Figure 4A shows an example where the 10-m transect is not representative of the smaller scale variance of the 100-m transect. This 10-m transect may also be deemed non-stationary because it represents scales less than the autocorrelation length scale and because its variance does not reach a sill.

Due to the unrepresentative nature of the 10-m transects, the rest of the discussion will focus on the spatial analysis of the 100-m transects. Power spectra of porosity of the forested and cultivated 100-m transects are presented in Fig. 5. Recall that the power spectrum partitions the total variance of a spatial series over a variety of spatial scales such that the integrated power spectrum is equal to the total variance. The power spectra of the forest A horizon is greater than the

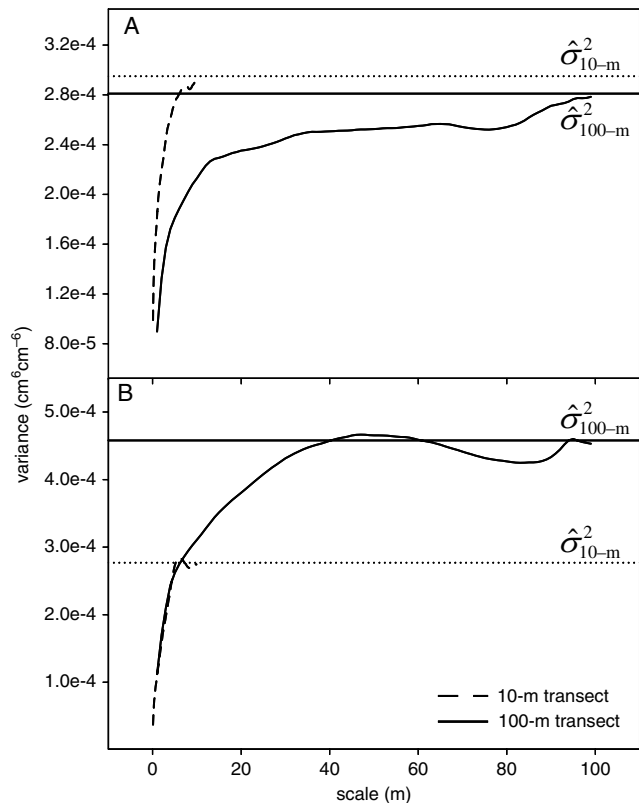


Fig. 4. Scale-dependent porosity variance of cultivated 10- and 100-m transects.

cultivated A horizon at all frequencies, which is a reflection of the fact that the total variance of the forest A horizon porosity estimates was nearly three times greater than the cultivated A horizon (Table 1). However, the porosity variance of the forested and cultivated transects are more similar at the smaller 2- to 3-m spatial scales than at the larger >5 -m spatial scales (Fig. 5A). Both forested and cultivated A horizon power spectra show decreasing variance with decreasing spatial scale (increasing frequency) from 100- down to 3.3-m spatial scales, but this decrease is more pronounced for the forested transect (Fig. 5A). The power spectra of forested and cultivated B horizon porosity are very similar. Total variance of the forested B horizon transect was only slightly greater than the cultivated transect (Table 1), as indicated by the slightly greater power from 10- down to the 3.3-m spatial scales (Fig. 5B).

Features of the scale-dependent variance of A and B horizon porosity (Figs. 3 and 4) are also reflected in the power spectra (Fig. 5). For example, the relatively gradual rise to a variance sill at a greater scale shown by the cultivated A horizon (Figs. 4A) is reflected in the relatively gradual decrease in variance from larger down to smaller spatial scales (Fig. 5A). Qualitatively, the decreasing nature of the power spectra (Fig. 5), from large scales down to small scales, indicates autocorrelated

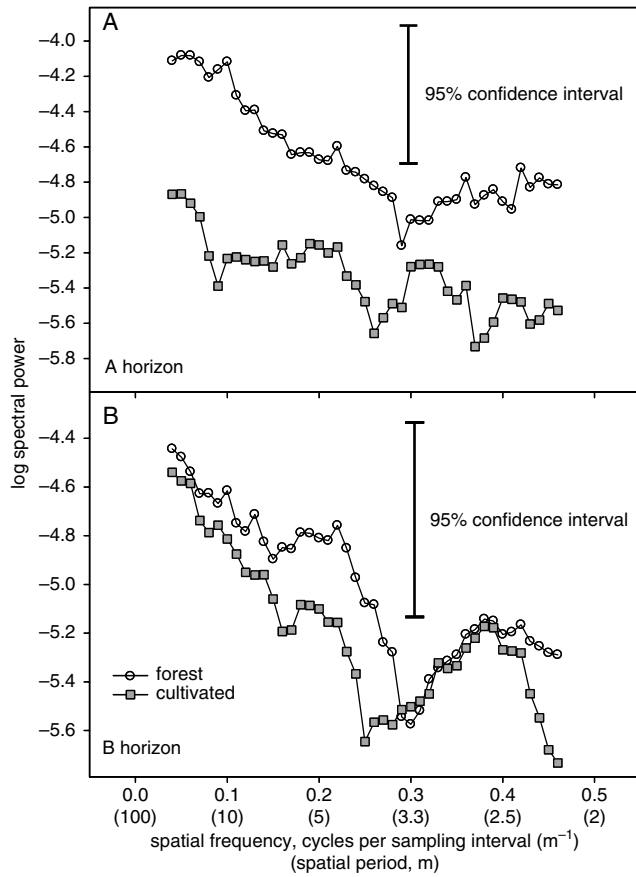


Fig. 5. Power spectra and A and B horizon porosity for forested and cultivated landscapes.

spatial patterns. The fact that the differences in power at large spatial scales (>10-m) and small scales (<3-m) of individual power spectra are greater than the 95% confidence interval indicates that the spatial patterns of A and B horizon porosity are significantly different from a random spatial pattern.

The covariance between A and B horizon 100-m transects as represented by a Pearson correlation matrix is presented in Table 2. Correlation coefficients (Table 2) indicate A and B horizon porosity are significantly correlated for the forested ($r = 0.58$; $P < 0.001$) and cultivated ($r = 0.35$; $P < 0.001$) transects. Coherency and cross-spectra, however, reveal differences in the scale-dependent covariance between A and B horizon porosity at the forested and cultivated sites (Fig. 6). Porosity estimates of the forested A and B horizons have highly significant coherency spectra estimates at large (>5-m) scales (Fig. 6A, circles), whereas the cultivated A and B horizon coherency spectrum did not show significant values at any scale (Fig. 6A, squares). Inspection of the cross-spectrum (i.e., total covariance as a function of scale) for the forested transect, indicates relatively high covariance (Fig. 6B, circles) at large scales of the forested transect. The high covariance at these large

Table 2. Pearson correlation coefficient matrix for 100-m transects

	Forest		Cultivated	
	A 100-m	B 100-m	A 100-m	B 100-m
<i>Forest</i>				
A 100-m	1			
B 100-m	0.58***	1		
<i>Cultivated</i>				
A 100-m	-0.17	-0.23*	1	
B 100-m	-0.17	-0.26**	0.35***	1

*, **, *** Significant at the 0.05, 0.01, and 0.001 probability levels, respectively.

scales was also where the forested A and B horizon porosity shows relatively high variability (Fig. 5), which adds further confidence to the significance of the coherency in these two patterns at these scales. That is, the large coherency values are a result of larger covariance between the spatial patterns rather than low variance of the individual spatial patterns (i.e., Eq. 5).

The A and B horizon porosity estimates for the cultivated site did not have significant coherency at any scale (Fig. 6A, squares) and consistently low covariance (Fig. 6B, circles). The spatial pattern of covariance for the cultivated transects (Fig. 6B) is very similar to the forested transects, but its overall magnitude is consistently lower than the forested transects. The spatial covariance at large scales (>3-m) is relatively high

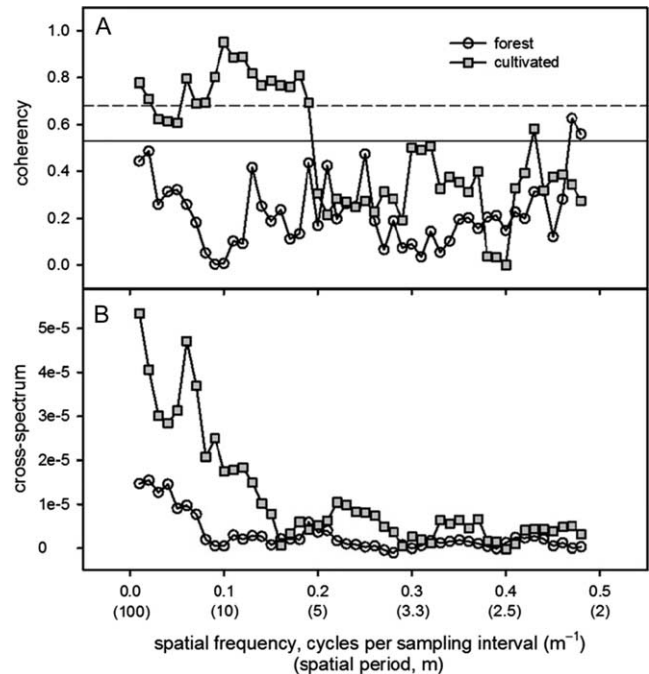


Fig. 6. A and B horizon porosity coherency (A) and covariance (cross-spectrum) (B). The solid and dashed lines in (A) represent the significant values of the coherency at the 95% and 99% confidence levels.

compared with other scales, but these scales are also where the cultivated A and B horizon porosity showed the highest variability (Fig. 5). Essentially the A and B horizon scale-dependent covariance decreased to a much greater degree than the variance of the individual horizons, accounting for the non-significant coherency values. Therefore, the fact that the Pearson correlation coefficient representing the integral in-phase covariance of cultivated A and B horizon porosity estimates is still significant ($r=0.35$; $P<0.001$) when the coherency is not, is likely a result of the decreased total variance in A horizon porosity (Table 1) rather than high absolute covariance between A and B horizons.

DISCUSSION

Based on the scale-dependent variance and covariance of the forested A and B horizon porosity estimates described above, it would appear that tillage has significantly altered the scale-dependent variance of porosity in the A horizon and the scale-dependent covariance of A and B horizon porosity from its original state as represented by the forested transects. Specifically, tillage has significantly reduced the total porosity and porosity variance of the A horizon (Table 1; Fig. 5A), and total covariance (Table 2) as well as spatial covariance between A and B horizon porosity at large scales (>5 m; Fig. 6). These observations are consistent with previous studies of tillage translocation and tillage-induced changes in soil physical properties. Comparison of native prairie and cultivated sites in Saskatchewan showed decreases in total porosity (i.e., increased bulk density), total soil organic carbon and significant changes in the spatial pattern of SOC after cultivation (Kachanoski et al. 1985; Pennock et al. 1994). While these examples are from grassland ecosystems, cultivation in forested ecosystems likely had similar impacts. Namely: (1) cultivation increases SOC mineralization, which may destroy soil structure and reduce total soil porosity in the plowed A horizon (da Silva et al. 1997; Kay and Munkholm 2004); and (2) tillage translocation physically moves soil in the direction of tillage and mixes soil horizontally and vertically (Kachanoski et al. 1985; Govers et al. 1994; Van Oost et al. 2006), which would likely decrease the A horizon total porosity variance and alter the spatial pattern of A horizon total porosity and the spatial covariance between A and B horizon porosity.

Initial changes in land use from natural to agricultural ecosystems involved clearing of vegetation and “catastrophic” plowing. The adjective “catastrophic” may seem like an exaggeration, but initial conversion of land to agriculture appears to significantly alter the variability and spatial patterns of surface properties, which influence ecosystem processes and pedogenesis. For example, Kachanoski et al. (1985) showed that 30 yr of cultivation significantly altered the spatial pattern of surface micro-topography by filling in micro-depressions with surrounding soil, which subsequently decreased the

overall spatial covariance between surface micro-topography and solum depth/mass. Van Wesemael et al. (2000), Dyck (2001) and Woods (2005) also showed that cultivation-induced erosion of convex areas and deposition in concave areas significantly influence local soil water balance. The filled-in concavities, which were historically focal points for ephemeral deep drainage events (as indicated by depletion of sulfates), became drier, more level landscape positions after cultivation (as indicated by a contemporary chloride tracer; Dyck 2001; Woods 2005). Tillage translocation in the landscape located in Spain studied by van Wesemael et al. (2000), exacerbated the spatial variability in solum depth and depth to bedrock, which significantly influenced soil moisture storage capacity. Thin soils in convexities became thinner, and thick soils in concavities became thicker as a result of tillage translocation. Based on these studies, cultivation reduced the local variability of micro-topography, soil water balance and the complex spatial covariance patterns between topography, soil morphology and hydrology that existed in the natural ecosystem. The relatively short time-scale (likely decades or less) for cultivation of effect significant changes such as these makes tillage a “catastrophic” event at least in the geological sense.

The observed differences between forested and cultivated spatial variance of A horizon porosity and spatial covariance between A and B horizon porosity are consistent with proposed hypothesis that these changes are tillage-induced. A tillage implement moving through the soil, tends to homogenize soil in the horizontal direction and sever any vertical continuity along the plane of the plowshare or cultivator shovel. This action essentially results in increasing the horizontal, but decreasing the vertical autocorrelation length scale of the property under observation. The observed differences in the scale-dependent variance of forested and cultivated A horizon porosity (Figs. 3A and 4A) indicate an increase in the variance sill from the 40-m spatial scale to the 70-m spatial scale. Power and coherency spectra are consistent with the scale-dependent variance showing a larger decrease in A horizon porosity variance and B horizon porosity covariance at large scales (>3 -m) after cultivation (Figs. 5A and 6). In terms of porosity, cultivation has essentially homogenized the A horizon and altered the spatial covariance between the A and B horizons that existed under the undisturbed forest ecosystem.

The observed scale-dependent covariance between A and B horizon porosity in the forested landscape (Fig. 6) is likely a result of the complex interactions and feedbacks between natural parent material variability (i.e., the initial spatial pattern of soil hydraulic properties), soil water balance (i.e., surface boundary conditions as influenced by the initial landscape topography), and pedogenic processes (i.e., weathering, translocation of solutes and colloids, SOM accumulation) that occurred during pedogenesis. The large scale covariance between A and B horizon porosity in the forested ecosystem

likely represents the scale at which pedogenic processes operated over the course of pedogenesis, which may be consistent with scales at which topography shows the greatest variance (i.e., Kachanoski and de Jong 1988). Furthermore, the observed scale-dependent covariance of A and B horizon porosity is an example of the difference between soil horizons and geological layers. Geological layers represent distinct changes in depositional environment, and the boundaries between them are often marked by a change in texture, a change in depositional structure(s), or an erosion surface. Soil horizons are usually formed from the same parent material, except in the special circumstance where horizons are used to mark a change in parent material. Soil horizons formed from the same parent material are essentially weathering interfaces and, therefore, there is some vertical continuity from one horizon into the next within a pedon and some horizontal continuity into adjacent pedons. The marked reduction in the scale-dependent covariance between A and B horizon porosity is likely a result of the physical disruption of the A/B horizon interface and translocation of particles within the A horizon interface.

The example of cultivation-induced changes in the spatial variance of A horizon porosity and the spatial covariance between A and B horizon porosity presented here is unique in that it potentially shows tillage impacts on the spatial covariance between soil physical properties above and below a soil horizon interface. Therefore, not only does tillage appear to alter the spatial variability of the soil water balance through alteration of surface morphology (surface boundary conditions; van Wesemael et al. 2000; Dyck 2001; Woods 2005), but also the hydraulic nature of the soil horizon interface (internal hydraulic properties) and their interactions. Furthermore, models of tillage translocation are spatio-temporal in nature (e.g., Kachanoski and de Jong 1984; Govers et al. 1994; Van Oost et al. 2006; Li et al. 2007; Li et al. 2008). In landscapes where cultivation occurs on an annual or more frequent basis, it is expected that topography and the spatial covariance between the surface horizon and underlying horizon properties and the nature of their scale-dependent covariance would be a function of time also. These changes would likely be most dramatic after initial conversion of the land and the following initial decade of cultivation.

This dynamic nature of cultivated landscapes introduces greater complexity into understanding water flow and solute transport processes, and emphasizes the significant impacts of human activities such as tillage on soil. Soil physical properties, such as porosity and pore size distribution, have been shown to significantly influence soil transport properties, such as hydraulic conductivity (e.g., Bouma 1989; Si and Zeleke 2005). If tillage changes surface boundary conditions and soil physical properties over time, then state soil transport properties like hydraulic conductivity are likely functions of time as well (e.g., Zhou et al. 2008; Alleto and

Coquette 2009). Possible temporal-dependent transport properties coupled with the expectation from theoretical stochastic continuum studies (e.g., Yeh et al. 1985a, b, c) that the spatial covariance between soil transport properties of overlying soil horizons significantly influences transport process at large-scales makes understanding and prediction of water flow and transport processes in soils exceedingly difficult. Furthermore, it makes the use of soil survey data and pedo-transfer functions (e.g., Bouma 1989) to predict state transport properties dubious.

In terms of pedogenesis, tillage represents a dramatic change from a “progressive” period of soil formation (Sommer et al. 2008), where pedogenic processes interacting with natural parent material variability and surface boundary conditions form soil profiles with spatially covariant soil horizons to a “regressive” period (Sommer et al. 2008), where tillage has irreversibly altered surface boundary conditions and internal soil hydraulic properties from the previous period. Therefore, soils in recently tilled landscapes (~100 yr) are likely unrepresentative of the conditions they were formed under, which potentially has great implications for soil classification systems.

CONCLUSIONS

The present study compared the spatially scale-dependent variability and covariance of A and B horizon porosity as measure from 10- and 100-m transects in forested and cultivated landscapes. While the integral covariance between A and B horizon porosity as represented by estimated Pearson correlation coefficients did not reveal any changes in the statistical significance of the linear relationship between A and B horizon porosity, this is a result of a marked decrease in A horizon porosity variance rather than a maintenance of A and B horizon porosity covariance after cultivation. A lower absolute A and B horizon covariance was also observed in the cultivated landscape. Coherency analysis was used to determine that the observed decrease in A and B horizon porosity covariance was concentrated at larger (> 5-m) spatial scales. This large-scale decrease in spatial covariance is consistent with scales at which tillage may alter soil physical properties and surface topography.

The present study supports the conceptual model of landscape/soil genesis recently presented by Sommer et al. (2008) of a relatively long period of “progressive” soil formation characterized by the traditional soil forming factors (climate, vegetation, parent material, topography, time) followed by a “regressive” period when removal of native vegetation and plowing changes topography (surface boundary conditions, soil water balance) and soil physical properties created during the “progressive” period. We propose that the conversion of land to agricultural use, which marks the transition from “progressive” to “regressive” periods of pedogenesis be considered a “catastrophic” event. By catastrophic, we mean that the spatial covariance patterns

between soils and surface topography and soil physical properties above and below horizon interfaces is dramatically changed within a relatively short period of time (i.e., decades).

Tillage-induced changes in spatial covariance patterns between soils and surface topography and soil physical properties above and below horizon interfaces likely affect surface boundary conditions, and internal soil hydraulic properties increasing the complexity of water flow and solute transport processes in cultivated landscapes. Further research into the time-scales associated with changing boundary conditions and state hydraulic and transport properties is required to assess the magnitude, variability and significance of these changes.

In terms of soil classification, the current pattern of soils in cultivated landscapes is likely not a reflection of the conditions they were formed under. Soil classification systems should be amended to reflect this reality.

Agriculture and Agri-Food Canada. 1998. The Canadian system of soil classification. Research Branch, Agriculture and Agri-Food Canada, Ottawa, ON.

Alleto, L. and Coquet, I. 2009. Temporal and spatial variability of soil bulk density and near-saturated hydraulic conductivity under two contrasted tillage management systems. *Geoderma* **152**: 85–94.

Bouma, J. 1989. Using soil survey data for quantitative land evaluation. *Adv. Soil Sci.* **9**: 177–213.

Brillinger, D. R. 1981. Time series: Data analysis and theory. 2nd ed. Holden Day, San Francisco, CA.

Carter, M. R. 1995. Spatial variability of soil porosity under reduced tillage in a Humo-Ferric Podzol. *Can. J. Soil Sci.* **75**: 149–152.

da Silva, A. P., Kay, B. D. and Perfect, E. 1997. Management versus inherent soil properties effects on bulk density and relative compaction. *Soil Tillage Res.* **44**: 81–93.

Duffy, C. J. and Gelhar, L. W. 1985. A frequency domain approach to water quality modeling in groundwater: Theory. *Water Resour. Res.* **21**: 1175–1184.

Dyck, M. F. 2001. Long-term solute transport under transient, semi-arid conditions. M.Sc. thesis, University of Saskatchewan, Saskatoon, SK. 200 pp.

Dyck, M. F. and Kachanoski, R. G. 2010. Spatial scale-dependence of preferred flow domains during infiltration in a layered field soil. *Vadose Zone J.* **9**: 385–396.

Gelhar, L. W. 1993. Stochastic subsurface hydrology. Prentice Hall, Englewood Cliffs, NJ.

Govers, G., Vandaele, K., Desmet, P., Poesen, J. and Bunte, K. 1994. The role of tillage in soil redistribution on hillslopes. *Eur. J. Soil Sci.* **45**: 469–478.

Jury, W. A. and Utermann, J. 1992. Solute transport through layered soil profiles: Zero and perfect travel time correlation models. *Transp. Porous Media* **8**: 277–297.

Lin, H., Bouma, J., Owens, P. and Vepraskas, M. 2008. Hydrogeology: Fundamental issues and practical applications. *Catena* **73**: 151–152.

Kachanoski, R. G. 1988. Processes in soils – from pedon to landscape. In T. Rosswall, R. G. Woodmansee, and P. G. Risser, eds. Scales and global change: Spatial and temporal variability in biospheric and geospheric processes. John Wiley, New York, NY.

Kachanoski, R. G. and de Jong, E. 1984. Predicting the temporal relationship between soil cesium-137 and erosion rate. *J. Environ. Qual.* **13**: 301–304.

Kachanoski, R. G. and de Jong, E. 1988. Scale dependence and the temporal persistence of spatial patterns of soil water storage. *Water Resour. Res.* **24**: 85–91.

Kachanoski, R. G., Rolston, D. E. and de Jong, E. 1985. Spatial variability of a cultivated soil as affected by past and present microtopography. *Soil Sci. Soc. Am. J.* **49**: 1082–1087.

Kay, B. D. and Munkhom, L. J. 2004. Management-induced soil structure degradation – Organic matter depletion and tillage. Pages 185–197 in P. Schjønning, S. Elmholt, and B. T. Christensen, eds. Managing soil quality: Challenges in modern agriculture. CABI Publishing International, Cambridge, MA.

Li, S., Lobb, D. A., Lindstrom, M. J. and Farenhorst, A. 2007. Tillage and water erosion on different landscapes in the northern North American Great Plains evaluated using ¹³⁷Cs technique and soil erosion models. *Catena* **70**: 493–505.

Li, S., Lobb, D. A., Lindstrom, M. J., Papiernik, S. K. and Farenhorst, A. 2008. Modeling tillage-induced redistribution of soil mass and its constituents within different landscapes. *Soil Sci. Soc. Am. J.* **72**: 167–179.

Pennock, D. J., Anderson, D. W. and de Jong, E. 1994. Landscape-scale changes in indicators of soil quality due to cultivation in Saskatchewan, Canada. *Geoderma* **64**: 1–19.

Percival, D. B. and Walden, A. T. 1993. Spectral analysis for physical applications: Multitaper and conventional univariate techniques. Cambridge University Press, New York, NY.

Protz, R., Fischer, J., Bolton, K., Shipitalo, S. E. and Lapalme, A. 1987. Spatial Dependence of selected properties of the Fox Sandy Loam. I. Sampling design and initial data. Techn. Memo. 87-2. Land Resource Science. University of Guelph, Guelph, ON.

Roth, K. 1995. Steady state flow in an unsaturated, two-dimensional, macroscopically homogeneous Miller-similar medium. *Water Resour. Res.* **31**: 2127–2140.

Si, B. C. 2008. Spatial scaling analyses of soil physical properties: A review of spectral and wavelet methods. *Vadose Zone J.* **7**: 547–562.

Si, B. C. and Zeleke, B. 2005. Wavelet coherency analysis to relate saturated hydraulic properties to soil physical properties. *Water Resour. Res.* **41**: W11424.

Sommer, M., Gerke, H. H. and Deumlich, D. 2008. Modelling soil landscape genesis – A “time split” approach for hummocky agricultural landscapes. *Geoderma* **145**: 480–493.

Ursino, N., Roth, K., Gimmi, T. and Flühler, H. 2000. Upscaling of anisotropy in unsaturated Miller-similar porous media. *Water Resour. Res.* **36**: 421–430.

Vanderborght, J., Kasteel, R. and Vereecken, H. 2006. Stochastic continuum transport equations for field-scale solute transport: Overview of theoretical and experimental results. *Vadose Zone J.* **5**: 184–203.

Van Oost, K., Govers, G., de Alba, S. and Quine, T. A. 2006. Tillage erosion: a review of controlling factors and implications for soil quality. *Prog. Phys. Geog.* **30**: 449–466.

van Wesemael, B., Mulligan, M. and Poesen, J. 2000. Spatial patterns of soil water balance on intensively cultivated hillslopes in a semi-arid environment: the impact of rock fragments and soil thickness. *Hydrol. Proc.* **14**: 1811–1828.

Van Wesenbeeck, I. J. and Kachanoski, R. G. 1991. Spatial scale dependence of in situ solute transport. *Soil Sci. Soc. Am. J.* **55**: 3–7.

Vereecken, H., Kasteel, R., Vanderborght, J. and Harter, T. 2007. Upscaling hydraulic properties and soil water flow processes in heterogeneous soils: A review. *Vadose Zone J.* **6**: 1–28.

Woods, S. A. 2005. Long-term field-scale transport of a chloride tracer under transient, semi-arid conditions. Ph.D. thesis, University of Saskatchewan, Saskatoon, SK. 306 pp.

Yeh, T. C. J., Gelhar, L. W. and Gutjahr, A. L. 1985a. Stochastic analysis of unsaturated flow in heterogeneous soils: 1. Statistically isotropic media. *Water Resour. Res.* **21**: 447–456.

Yeh, T. C. J., Gelhar, L. W. and Gutjahr, A. L. 1985b. Stochastic analysis of unsaturated flow in heterogeneous soils: 2. Statistically anisotropic media with variable α . *Water Resour. Res.* **21**: 457–464.

Yeh, T. C. J., Gelhar, L. W. and Gutjahr, A. L. 1985c. Stochastic analysis of unsaturated flow in heterogeneous soils: 3. Observations and applications. *Water Resour. Res.* **21**: 465–471.

Zhou, X., Lin, H. S. and White, E. A. 2008. Surface soil hydraulic properties in four soil series under different land uses and their temporal changes. *Catena* **73**: 180–188.